

# Circulation

JOURNAL OF THE AMERICAN HEART ASSOCIATION

American Heart  
Association®   
*Learn and Live*™

## **Optical mapping of repolarization and refractoriness from intact hearts**

IR Efimov, DT Huang, JM Rendt and G Salama

*Circulation* 1994;90:1469-1480

Circulation is published by the American Heart Association, 7272 Greenville Avenue, Dallas, TX  
72514

Copyright © 1994 American Heart Association. All rights reserved. Print ISSN: 0009-7322. Online  
ISSN: 1524-4539

The online version of this article, along with updated information and services, is  
located on the World Wide Web at:  
<http://circ.ahajournals.org>

Subscriptions: Information about subscribing to *Circulation* is online at  
<http://circ.ahajournals.org/subscriptions/>

Permissions: Permissions & Rights Desk, Lippincott Williams & Wilkins, a division of Wolters  
Kluwer Health, 351 West Camden Street, Baltimore, MD 21202-2436. Phone: 410-528-4050. Fax:  
410-528-8550. E-mail:  
[journalpermissions@lww.com](mailto:journalpermissions@lww.com)

Reprints: Information about reprints can be found online at  
<http://www.lww.com/reprints>

# Optical Mapping of Repolarization and Refractoriness From Intact Hearts

Igor R. Efimov, PhD; David T. Huang, MD; James M. Rendt, PhD; Guy Salama, PhD

**Background** Heterogeneities of repolarization (R) across the myocardium have been invoked to explain most reentrant arrhythmias. The measurement of refractory periods (RPs) has been widely used to assess R, but conventional electrode and extrastimulus mapping techniques have not provided reliable maps of RPs.

**Methods and Results** Guinea pig hearts were stained with a voltage-sensitive dye to measure fluorescence (F) action potentials (APs) from 124 sites with a photodiode array. AP duration (APD) was defined as the time between depolarization ( $dF/dt$ )<sub>max</sub> and R time points (ie, the time when AP returns to baseline or some percent thereof). However, R time points are difficult to determine because AP downstrokes are often encumbered by drifting baselines and motion artifacts, which make this definition ambiguous. In optical and microelectrode recordings, the second derivative of AP downstrokes is shown to contain an easily detected, unique local maximum. The

correlation between the position of this maximum ( $d^2F/dt^2$ )<sub>max</sub> and R has been tested during altered AP characteristics induced by changes in cycle length, ischemia, and hypoxia. Under these various modifications of the AP, the time points of ( $d^2F/dt^2$ )<sub>max</sub> fell at  $97.0 \pm 2.1\%$  of recovery to baseline. Extrastimulus techniques applied to (1) isolated myocytes, (2) intact hearts, and (3) mathematical simulations indicated that ( $d^2V/dt^2$ )<sub>max</sub> coincided with the effective RPs of APs. The coincidence of RPs and ( $d^2V/dt^2$ )<sub>max</sub> was valid within 5 milliseconds, for resting potentials of  $-75$  to  $-90$  mV and extrastimuli three times threshold voltage.

**Conclusions** Thus, optical APs and ( $d^2F/dt^2$ )<sub>max</sub> can be used to map activation, R, and RPs with AP recordings from a single heartbeat. (*Circulation*. 1994;90:1469-1480.)

**Key Words** • mapping • electrophysiology • action potentials

Spatial heterogeneities in repolarization have been proposed to explain the initiation of arrhythmias in cardiac tissue.<sup>1</sup> Theoretically, a unidirectional block can arise in regions containing abrupt variations of repolarization.<sup>2</sup> Under certain conditions, these variations can lead to wavefront fractionation and reentry. However, reliable experimental tests of this hypothesis have not been achieved.

The major obstacle to testing this hypothesis is the lack of a practical technique to measure distributions of repolarization with sufficient spatial and temporal resolution. The most common approach to map repolarization pathways is indirect, through measurements of refractory periods.<sup>3</sup> Maps of refractoriness are conventionally measured by combining multiple extracellular electrode recordings with premature extrastimulus techniques.<sup>4</sup> The heart is paced at a basic rate ( $S_1$ ), and a premature stimulus ( $S_2$ ) is applied with a variable coupling interval ( $S_2-S_1$ ). A disadvantage of this approach is that the extrastimulus must be tested with variable delays,  $S_2-S_1$ , to determine the refractory period at each recording site and the process must be repeated at each electrode site to measure distributions of refractory periods. Maps of refractory periods derived by this approach are time-consuming and assume that the refractory period measured at one site did not vary while the measurements were repeated at other

sites. As a result, such mapping measurements cannot be practically repeated under different physiological conditions without compromising both spatial and temporal resolution. Another difficulty is that the definition of refractory period depends on the amplitude, duration, and polarity of the stimulating current. Michelson et al<sup>5</sup> studied refractory periods in normal and ischemic myocardium and pointed out the difficulties inherent in choosing a standardized threshold current for the definition of refractory periods.

Intracellular microelectrodes provide accurate measurements of repolarization but are not practical for simultaneous measurements from multiple sites because of technical difficulty of maintaining multiple stable recordings.

Suction electrodes have been used to measure action potential (AP) durations (APDs) and refractory periods by monitoring conduction time delays between two sites.<sup>6</sup> Premature stimuli delivered near the relative refractory period increased conduction time delays because the extra AP propagated at slower conduction velocity. Refractory periods could thus be accurately determined and were shown to coincide with AP repolarizations. However, suction electrodes are not practical for simultaneous recordings of refractory periods at multiple sites and may produce unreliable recordings caused by tissue damage.<sup>6</sup>

Signal processing techniques have been proposed to estimate repolarization by use of unipolar electrograms by correlating the most rapid increase in voltage ( $dV/dt$ )<sub>max</sub> near the peak of the T wave to the repolarization of the local AP.<sup>7</sup> Millar et al<sup>8</sup> defined an "activation-recovery interval" as the time difference between the

Received January 31, 1994; revision accepted May 23, 1994.

From the Department of Cell Biology and Physiology, University of Pittsburgh (Pa) School of Medicine.

Correspondence to Guy Salama, Department of Cell Biology and Physiology, University of Pittsburgh School of Medicine, Pittsburgh, PA 15261.

$(dV/dt)_{\min}$  (activation time) and  $(dV/dt)_{\max}$  near the peak of the T wave (repolarization time). Experimental<sup>8</sup> and theoretical<sup>9</sup> studies suggested that refractory periods were correlated with activation-recovery intervals. However, this correlation remained empirical, was strongly dependent on the shape, polarity, and kinetics of the T wave, and failed for multiphasic T waves. Ultimately, it proved to be of limited use because the amplitudes and kinetics of T waves were too variable to determine refractory periods.

We have previously used voltage-sensitive dyes and imaging technique to simultaneously measure 124 APs from the epicardium of perfused hearts.<sup>10</sup> In preliminary reports, we described signal processing techniques to uniquely identify the repolarization time points of fluorescence (F) APs through  $(d^2F/dt^2)_{\max}$  of their downstroke.<sup>11</sup> The algorithm was effective to measure repolarization time points even in optical AP recordings containing substantial distortions caused by movement artifacts. The method made it possible to measure heterogeneities of repolarization and APDs in normal and hypoxic hearts during abrupt cycle length shortening.<sup>12</sup>

The present report investigates the physiological significance of this inflection point detected during AP downstrokes by theoretical and experimental approaches. The data show that  $(d^2F/dt^2)_{\max}$  provides a reliable measurement of AP repolarization and is coincident with AP refractory period under physiological resting potentials. Preliminary reports of these findings have appeared in abstract form.<sup>11,13</sup>

## Methods

### Preparations

Guinea pigs of either sex weighing between 350 and 450 g were anesthetized with an intraperitoneal injection of sodium pentobarbital (Nembutal, 30 mg/kg). The hearts were rapidly excised, rapidly cannulated at the aorta (within 60 seconds), and retrogradely perfused in a modified Langendorff apparatus. The Krebs-Ringer's perfusate consisted of (in mmol/L) NaCl 130, KCl 4.75,  $CaCl_2$  1.0,  $MgSO_4$  1.2,  $NaHCO_3$  12.5, and glucose 5.0. The solution was continuously gassed with 95%  $O_2$ /5%  $CO_2$ , pH adjusted to  $7.4 \pm 0.1$  with  $NaHCO_3$ . Temperature was maintained at  $35 \pm 1^\circ C$  with a thermistor probe and a heat-exchange coil. A perfusion pressure of 80 to 90 cm  $H_2O$  was maintained from the beginning of the experiment with variable flow rate ( $\approx 2 \text{ mL} \cdot \text{min}^{-1} \cdot \text{g}^{-1}$  heart wt). More detailed methods describing the perfusion setup, the staining procedure, the heart chamber, optics, and computer hardware and software were previously reported<sup>10,12,14</sup> and are briefly restated below.

Hearts were paced at a fixed cycle length, typically 300 or 350 milliseconds, with a bipolar  $Ag^+/AgCl$  electrode placed on the epicardium. The output of the pacer was adjusted to 1.5 times the threshold voltage. A custom-designed perfusion chamber was used for studying intact guinea pig hearts. The preparation was held in place by a glass window at the front of the chamber and side and rear pads to minimize gross movement of the heart during contractions. Bipolar surface electrogram recordings were measured by use of Teflon-coated silver wires (250- $\mu\text{m}$  diameter), with  $Ag^+/AgCl$  at the exposed tip of the wires and a 0.5-mm gap between the two wires. These sensing electrodes were sutured or glued to the epicardium to maintain stable recordings. The left epicardium was in contact with the glass of the front window to reduce the curvature of the ventricle and gross movement during contractions of the heart. The heart in the chamber was immersed in perfusate

### Staining Procedures

A styryl dye, RH-421 (S-1108, lot 2711-2, Molecular Probe), was used as the voltage-dependent fluorescent probe. When bound to the sarcolemma, RH-421 fluorescence was measured at wavelengths above the 645-nm cutoff filter when excited with a  $520 \pm 20$ -nm interference filter. The dye exhibited a large fractional decrease in fluorescence of 6% to 9% per 100 mV depolarization such that the voltage-dependent responses appeared as upside-down APs.<sup>14</sup> The signals were automatically inverted under software to appear as rightside-up APs. This dye was chosen because it did not provoke detectable pharmacological effects, remained optically stable in solution, and exhibited optical APs with high signal-to-noise ratios (up to 250:1) for 2 to 4 hours.

Hearts were stained by gradual injection of 50 to 100  $\mu\text{L}$  from a 3 mmol/L stock solution of dye into a 5-mL bubble trap situated directly above the aortic cannula. The final dye concentration was approximately 2.5  $\mu\text{mol/L}$ , and 15 to 20 minutes was allowed for the staining to be completed. The procedure resulted in homogeneous staining throughout the heart because the dye was efficiently delivered via coronary vessels. In experiments lasting more than 4 hours, photobleaching and/or dye washout reduced the signal amplitudes; in such cases, hearts were occasionally restained to restore the original signal-to-noise ratio.

The experiments described in this study were based on a total of 20 guinea pig hearts. Six were used to map repolarization with voltage-sensitive dyes, 2 to prepare isolated myocytes for single-cell measurements of refractory periods, 6 for measurements during hypoxia, and 6 during ischemia. This investigation conformed with the Guide for the Care and Use of Laboratory Animals published by the US National Institutes of Health (NIH publication No 85-23, revised in 1985).

### Instrument Setup

Details of the optical and recording apparatus have been described elsewhere.<sup>10</sup> The perfusion chamber containing the Langendorff-perfused heart was mounted on a micromanipulator and positioned along the optical axis of a photodiode array scanning apparatus. Light from two 45-W tungsten-halogen lamps was collimated, passed through a  $520 \pm 20$ -nm interference filter, reflected off a  $45^\circ$  dichroic mirror, and focused on the left epicardium of the heart with a 35-mm camera lens (50 mm, f 1:1.4, Nikon). Epifluorescent light from the stained heart was collected, projected through a 645-nm cutoff filter, and focused to form an image of the heart on a  $12 \times 12$ -element photodiode array. The photodiode array consisted of 144 square diode elements, with each diode having dimensions of  $1.4 \times 1.4$  mm separated by 0.1 mm of dead space. Of the 144 available diodes, 124 diodes were monitored; five elements from each corner were disregarded. The distances between the preparation, the lens, and the array could be varied and thus, the image of the heart falling on the array could be magnified by 1.5 to 6 times. In the present study, APs were recorded from a  $12 \times 12$ -mm<sup>2</sup> region of the epicardium. The depth of field of the optics restricted the detection of dye fluorescence to a depth of 144  $\mu\text{m}$  from the surface of the epicardium.<sup>14</sup>

### Signal Acquisition

A scan of data acquisition consisted of 128 simultaneously recorded traces: 124 optical plus 4 instrumentation channels. The multiplexed instrumentation channels monitored the stimulus pulses, two surface electrogram signals located on the atrium and ventricle, and in some experiments, left ventricular pressure by use of a latex balloon inserted in the left ventricular cavity and a Statham pressure transducer (model P-10). A scan consisted of a continuous recording of these 128 channels for 1.2 to 34 seconds. The photocurrents from 124 diodes were

kHz per channel, 8 bits per sample), and stored in a memory buffer of a Digital Equipment Corp PDP 11-73 computer.

### Experiments on Isolated Myocytes

Guinea pig myocytes were isolated with collagenase and pronase as previously described.<sup>15</sup> Current clamp measurements were performed with an Axoclamp 1D. Data were collected at a 5-kHz sampling rate. Patch pipettes were filled with a solution of the following composition (in mmol/L): KCl 140, HEPES 10, MgATP 5, EGTA 10 at pH 7.25. Cells were superfused with an external solution containing (in mmol/L): NaCl 130, KCl 5, MgCl<sub>2</sub> 1, CaCl<sub>2</sub> 2, HEPES 10, glucose 5, pH 7.35 at 37°C.

### Computer Simulation

Computer simulations were performed with mathematical models of electrical activity in ventricular myocardial fiber.<sup>16</sup> The Beeler-Reuter model is a system of first-order nonlinear differential equations of the Hodgkin-Huxley type. To solve the system, an implicit scheme with time step  $\Delta t=0.01$  millisecond was used. Activation and inactivation parameters in a model of Hodgkin-Huxley type obey the usual first-order equation

$$dy/dt = \alpha_y(1-y) - \beta_y(y)$$

where  $y$  is a parameter ( $m$ ,  $h$ , etc),  $t$  is time (milliseconds), and  $\alpha_y$  and  $\beta_y$  are rate constants (milliseconds). If we call  $y$  the parameter value at the  $n$ th time step ( $\Delta t$ ), the finite-difference equation for the time derivative yields

$$(y^{n+1} - y^n)/\Delta t = \alpha_y(1 - y^{n+1}) - \beta_y(y^{n+1})$$

which can be rewritten to

$$y^{n+1} = (y^n + \alpha_y \Delta t) / [1 + (\alpha_y + \beta_y) \Delta t]$$

The equation for membrane potential is

$$dE/dt = \Sigma i/C = \Sigma g(E - E_r)/C$$

where  $E$  is the membrane potential (millivolts),  $i$  is ionic currents ( $\mu A/cm^2$ ), and  $C$  is the membrane capacitance ( $\mu F/cm^2$ ). The finite-difference equation for the time derivative in this case is

$$(E^{n+1} - E^n)/\Delta t = -(1/C)\Sigma g(E^{n+1} - E_r)$$

which takes the form

$$E^{n+1} = [E^n + (\Delta t/C)\Sigma g E_r] / [1 + (\Delta t/C)\Sigma g]$$

Stimulations of a model cell with normal Beeler-Reuter parameters were made by applying an external current pulse with amplitude  $i_{ext}=12 \mu A/cm^2$  and duration  $\Delta t=5$  milliseconds. Computations were performed on IBM/PC-386 clone and the CRAY C90 of the Pittsburgh Supercomputing Center. Programs were written with Borland C++ compiler.

## Results

### Second Derivative of the Cardiac AP

A signal-processing technique was used to detect the activation (depolarization) and recovery (repolarization) time points of fluorescence (F) APs. The activation time point was defined as the maximum first derivative  $(dF/dt)_{max}$  of the AP upstroke. The recovery time point was defined as the maximum second derivative of the AP downstroke,  $(d^2F/dt^2)_{max}$ , because the second derivative of the cardiac AP was found to exhibit a local maximum between the most negative slope of the AP downstroke and the return to baseline.<sup>11-13</sup> Fig 1

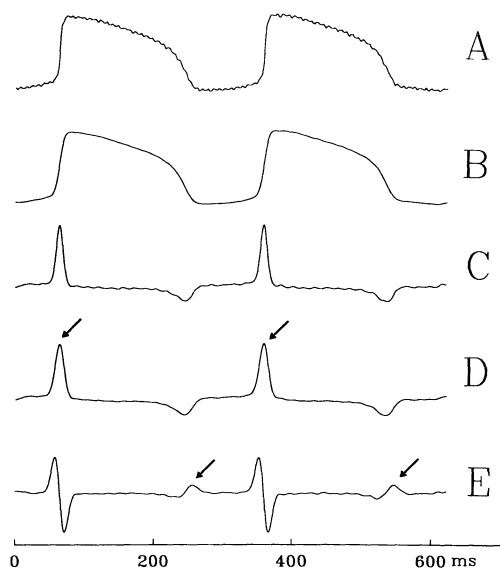


Fig 1. Tracings showing signal processing of optical action potentials (APs) to resolve depolarization and repolarization time points. A, An optical AP was recorded (at 1.3 kHz) from a  $1 \times 1$ -mm area of left epicardium from a perfused guinea pig heart. The voltage-dependent optical signal corresponded to a fractional decrease of fluorescence of 8%. B, The fluorescence (F) AP shown in (A) was filtered with a boxcar of 8 milliseconds' duration. C, Its first time derivative was obtained after filtration from trace B. D, Trace C was filtered with a 23-millisecond boxcar, and the time of depolarization was taken at the time point of  $(dF/dt)_{max}$  of the AP upstroke (arrows on trace D). E, The time derivative of trace D is shown; note the unique peak that coincides with the end of the repolarization phase of the AP. The repolarization time point was taken at  $(d^2F/dt^2)_{max}$  (arrows on trace E).

photodiode array (Fig 1A). The diode recorded the sum of voltage-dependent optical response of a group of cells (viewed by the diode) contained in a  $1 \times 1$ -mm<sup>2</sup> area of left epicardium and a depth of 144  $\mu m$ . The recording contained high-frequency noise (Fig 1A), which was filtered with a boxcar of 8 milliseconds' duration to obtain Fig 1B. The depolarization time point of an AP recorded with an intracellular electrode is conventionally defined at the maximum first derivative of the AP upstroke,  $(dV/dt)_{max}$ . For optical APs, the time point of depolarization was also defined as the maximum first derivative of the fluorescence AP upstroke  $(dF/dt)_{max}$  because it corresponded to the time when most of the cells viewed by a diode were depolarizing. The depolarization time point was detected by taking the first derivative of Fig 1B to obtain Fig 1C  $(dF/dt)_{max}$ , at arrows). The first derivative trace (Fig 1C) was filtered with a 23-millisecond boxcar to generate Fig 1D before taking the second derivative to generate Fig 1E. The repolarization time point is typically defined as the recovery of the AP back to baseline, which provides an accurate method to measure AP duration whenever the downstroke has a large negative slope and returns abruptly to its resting potential. When the downstroke returns gradually to baseline, repolarization is alternatively defined as a percentage of recovery to baseline. These definitions are often not suitable for optical recordings because movement artifacts distort the repolarization phase (see Fig 2). Consequently, the repolarization time point was defined as the time point of the maximum second derivative of the AP downstroke,  $(d^2F/dt^2)_{max}$ , because it coincided with the end of the repolarization phase of the AP (arrows on trace E).



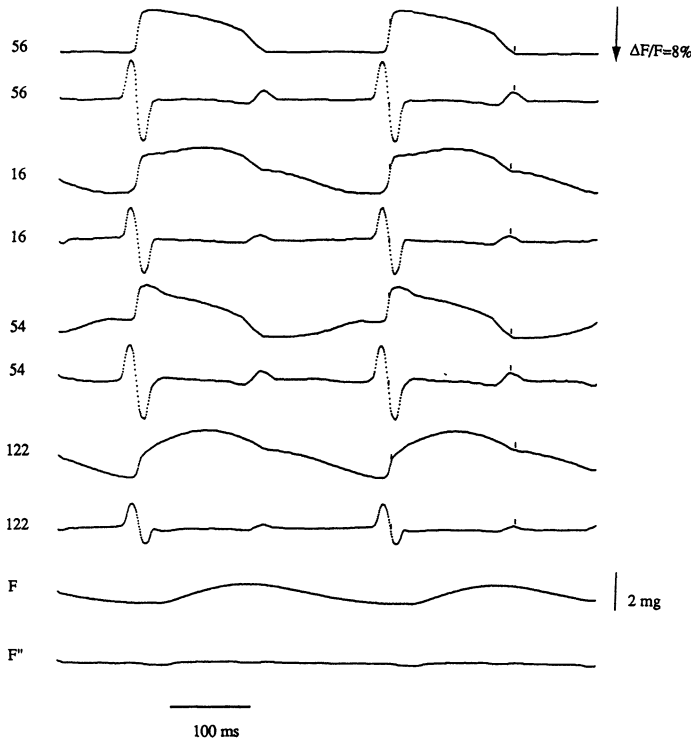


Fig 2. Tracings show that  $(d^2F/dt^2)_{max}$  of action potential (AP) downstrokes are not distorted by motion artifacts. Four of 124 simultaneously recorded APs are shown, and each is followed by its second derivative determined as described in Fig 1. The AP signal from diode 56 was chosen as an example of an optical AP with negligible motion artifact. APs from diodes 16, 54, and 122 were selected for their substantial levels of motion artifacts. Their second derivatives,  $d^2F/dt^2$ , show prominent peaks at the repolarization time points of the APs. The computer algorithm automatically determined  $(d^2F/dt^2)_{max}$  and placed a "tick" mark at the calculated repolarization time point. The algorithm identified unique repolarization time points for  $95 \pm 2\%$  of the APs recorded by the array. Developed force was measured with a balloon inserted into the left ventricular cavity. Peak developed force occurred during or just before the rapid phase of repolarization, and developed force was substantial during the repolarization phases, which accounted for the movement artifact. However, the second derivative of the force (and most likely movement artifacts) was relatively flat during repolarization.

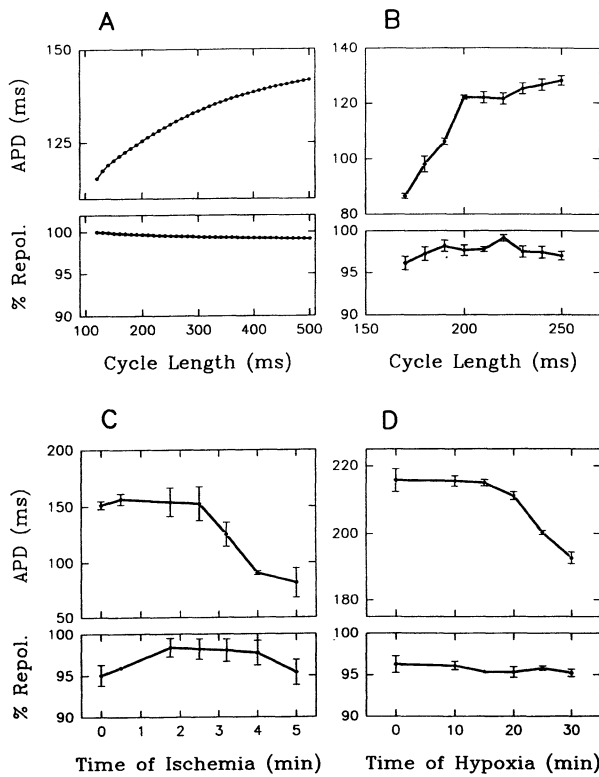


Fig 3. Graphs showing that  $(d^2F/dt^2)_{max}$  coincides with action potential (AP) repolarization under various physiological and pathological conditions. The correlation between  $(d^2F/dt^2)_{max}$  and repolarization was tested in simulations of the AP by use of the Beeler-Reuter model and with optical recordings under various conditions. AP durations (APD) were defined as the time difference  $dF/dt_{max} - (d^2F/dt^2)_{max}$  of AP upstrokes and downstrokes. APs recorded by 12 of the 124 diodes were chosen for their negligible levels of movement artifact and were analyzed to correlate their percent repolarization (or recovery back to baseline) to the time point of  $(d^2F/dt^2)_{max}$ . Percent of repolarization was measured at the time point of  $(d^2F/dt^2)_{max}$ . For mathematical simulations, APDs were defined in the same way; that is, as the difference between  $(dV/dt)_{max}$  and  $(d^2V/dt^2)_{max}$ . A, APs were generated from Beeler-Reuter simulations and their APDs measured as a function of cycle length (CL) (top trace). The percent repolarization at the time point of  $(d^2V/dt^2)_{max}$  was determined for APs at each CL and plotted in the lower graph. The data show that as APDs increased from 115.46 to 141.71 milliseconds with CLs increasing from 120 to 500 milliseconds, the time point of  $(d^2V/dt^2)_{max}$  coincided with  $99.46 \pm 0.23\%$  (mean  $\pm$  SD) repolarization back to baseline. B, The equivalent analysis was repeated with optical APs from the left epicardium of guinea pig hearts paced at different cycle lengths. A bipolar stimulating electrode was placed on the right atrium to pace the heart at faster rates than the intrinsic pacemaker rate. APDs from 12 central diodes were analyzed to test the correlation between  $(d^2F/dt^2)_{max}$  and the percent repolarization. Top plot, Each data point represents the mean APD  $\pm$  SD for 12 APs recorded at a given cycle length. APDs increased from 94.09 to 130.39 milliseconds with increasing cycle lengths from 170 to 250 milliseconds. Bottom plot, Each data point represents the averaged percent repolarization  $\pm$  SD at the times that correspond to  $(d^2F/dt^2)_{max}$  of the 12 APs;  $(d^2F/dt^2)_{max}$  occurred at  $96.14 \pm 0.82\%$  repolarization (mean  $\pm$  SD). C and D, Same analysis as in B except that APDs and percent repolarization were plotted as a function of time of ischemia (C) and hypoxia (D). Preparations were paced at CL=350 milliseconds. Ischemia experiments were carried out at 35°C, APDs decreased from 156.52 to 81.42 milliseconds in 5 minutes of ischemia, and  $(d^2F/dt^2)_{max}$  fell at  $96.96 \pm 1.44\%$  of repolarization. Hypoxia experiments were carried out at 23°C, APDs decreased from 215 to 192 milliseconds in 30 minutes, and  $(d^2F/dt^2)_{max}$  fell at a similar percent repolarization of  $95.67 \pm 0.43\%$ . The higher percent repolarization in theoretical compared with the experimental results was attributed

# Explore Litigation Insights

Docket Alarm provides insights to develop a more informed litigation strategy and the peace of mind of knowing you're on top of things.

## Real-Time Litigation Alerts



Keep your litigation team up-to-date with **real-time alerts** and advanced team management tools built for the enterprise, all while greatly reducing PACER spend.

Our comprehensive service means we can handle Federal, State, and Administrative courts across the country.

## Advanced Docket Research



With over 230 million records, Docket Alarm's cloud-native docket research platform finds what other services can't. Coverage includes Federal, State, plus PTAB, TTAB, ITC and NLRB decisions, all in one place.

Identify arguments that have been successful in the past with full text, pinpoint searching. Link to case law cited within any court document via Fastcase.

## Analytics At Your Fingertips



Learn what happened the last time a particular judge, opposing counsel or company faced cases similar to yours.

Advanced out-of-the-box PTAB and TTAB analytics are always at your fingertips.

## API

Docket Alarm offers a powerful API (application programming interface) to developers that want to integrate case filings into their apps.

## LAW FIRMS

Build custom dashboards for your attorneys and clients with live data direct from the court.

Automate many repetitive legal tasks like conflict checks, document management, and marketing.

## FINANCIAL INSTITUTIONS

Litigation and bankruptcy checks for companies and debtors.

## E-DISCOVERY AND LEGAL VENDORS

Sync your system to PACER to automate legal marketing.